He-Fang Wang[1]
Yi-Zhou Zhu[2]
Jian-Ping Lin[1]
Xiu-Ping Yan[1]

[1]Research Center for Analytical Sciences, College of Chemistry, Nankai University, Tianjin, P. R. China
[2]State Key Laboratory and Institute of Elemento-Organic Chemistry, Nankai University, Tianjin, P. R. China

Received June 5, 2007
Revised July 19, 2007
Accepted August 23, 2007

Research Article

Fabrication of molecularly imprinted hybrid monoliths *via* a room temperature ionic liquid-mediated nonhydrolytic sol–gel route for chiral separation of zolmitriptan by capillary electrochromatography

A room temperature ionic liquid (RTIL)-mediated nonhydrolytic sol–gel (NHSG) protocol was explored for the fabrication of new molecularly imprinted silica-based hybrid monoliths for chiral separation of a basic template zolmitriptan by CEC. The RTIL-mediated NHSG protocol involved free-radical copolymerization and NHSG process. Three carboxylic acids (trifluoromethyl acrylic acid, cinnamic acid, and methacrylic acid (MAA)) were examined as both the functional monomers and the catalysts for the NHSG condensation of methacryloxypropyltrimethoxysilane (MPTMS) to form silica-based framework. RTIL was incorporated to reduce gel shrinkage and also to act as the pore template. The effects of carboxylic acids and RTIL on the performance of the silica-based hybrid molecularly imprinted polymer (MIP) monoliths were investigated in detail to realize excellent chiral recognition and to give new insights into the mechanism of the RTIL-mediated NHSG strategy. Excellent chiral separation of (*R*)/(*S*)-zolmitriptan was achieved when the molar ratio of MAA to MPTMS was 1:4 and 1:2 with RTIL involved. The synergism of the free-radical copolymerization of the C=C bond of carboxylic acids and MPTMS with the NHSG condensation of MPTMS catalyzed by the carboxylic acids was demonstrated. The incorporation of RTIL increased porosity, and hence improved selectivity of the prepared hybrid monoliths.

Keywords:
Capillary electrochromatography / Hybrid molecularly imprinted polymers / Nonhydrolytic sol–gel process / Room temperature ionic liquid / Zolmitriptan
DOI 10.1002/elps.200700402

1 Introduction

Development of novel materials for chiral recognition has become increasingly important due to the significance of chiral separation, especially in the field of life sciences [1, 2]. Molecularly imprinted polymers (MIPs) with a memory for the template have the potential to be powerful materials in the separation of chiral compounds, predicting not only the recognition ability but also the elution order [3–7]. Organic-polymer-based MIPs are extensively applied due to their excellent pH stability and the easy availability of various monomers [8–12], but they may shrink or swell when exposed to different organic solvent, and thus considerably cause the deformation of the MIP receptors and decrease the recognition ability towards the template [13]. Silica-based MIPs are also widely studied since the silica matrix can offer excellent mechanical strength and good solvent resistance. However, silica-based MIPs are often prepared by conventional hydrolytic sol–gel process [14–22], which often require curing and ageing at high temperature, and thus inevitably result in the poor properties of MIPs due to the cracking and the shrinkage of MIPs during drying, especially in the case of the MIP monolithic column [23]. For these reasons, earlier works on MIP monoliths in CEC focused more on organic-polymer-based and less on the silica-based hybrid [8–12]. An alternative approach to prepare the silica-based MIP monoliths is to

Correspondence: Professor Xiu-Ping Yan, Research Center for Analytical Sciences, College of Chemistry, Nankai University, 94 Weijin Road, Tianjin 300071, P. R. China
E-mail: xpyan@nankai.edu.cn
Fax: +86-22-23506075

Abbreviations: BMIM$^+$BF$_4^-$, 1-butyl-3-methylimidazolium tetrafluoroborate; **BMIM$^+$PF$_6^-$,** 1-butyl-3-methylimidazolium hexafluorophosphate; **MAA,** methacrylic acid; **MIP,** molecularly imprinted polymer; **TFMAA,** trifluoromethyl acrylic acid; **MPTMS,** methacryloxypropyltrimethoxysilane; **NHSG,** nonhydrolytic sol–gel; **RTIL,** room temperature ionic liquid

anchor the MIP film coating covalently on the surface of a pre-prepared monolithic silica column [24] and fast association/dissociation kinetics of the analytes with the MIP monoliths was expected. However, curing and ageing at 330°C was still required for preparing the monolithic silica column [24].

A promising way to prepare the silica-based MIPs without curing and ageing is the nonhydrolytic sol–gel (NHSG) process due to no or little water involved. Another way to reduce the shrinkage and subsequent matrix collapse during formation of the gels is to use the nonvolatile drying control chemical additives [25]. Room temperature ionic liquid (RTIL) is a good choice due to its generally negligible vapor pressure. RTIL is also anticipated to control over the structural properties of the resultant MIPs, particularly with respect to pore size, structure, and distribution, owing to the readily modifiable and controllable characteristics of RTIL [25]. Consequently, the novel RTIL mediated NHSG methodology is expected as a sound route to prepare porous silica-based hybrid MIP monoliths for chiral separation [26]. Moreover, this method also offer the potential to owe the advantage of surface imprinting since the resultant MIPs would have the characteristics of smaller particles and higher porosity with smaller pores and a smaller pore size distribution due to the incorporation of RTIL [25, 26].

In our preliminary communication [26] was only an acidic drug ((*S*)-naproxen) used as template to demonstrate the applicability of the novel RTIL-mediated NHSG methodology as the acidic template can catalyze the NHSG reaction itself, and can bind with the functional monomer (methacrylic acid, MAA) *via* hydrogen bonding and the hydrophobic interaction. However, when a basic template is involved, the ionic interaction would be dominant and part of carboxylic acids such as MAA would be consumed, and the NHSG process would be different since the basic template cannot catalyze the NHSG reactions. Another challenge for a basic template is the pH stability of the silica-based hybrid MIPs since the pH value of the separation mobile phase for a basic drug would be higher when the resultant MIP monoliths are evaluated by CEC. Therefore, a question arises, *i.e.*, whether is the RTIL-mediated NHSG methodology also applicable when a basic drug is used as the template?

The main purposes of the present work are to explore the feasibility of the RTIL-mediated NHSG methodology for fabricating new molecularly imprinted hybrid monoliths for chiral recognition of basic drugs, and to elucidate the possible mechanism of the RTIL-mediated NHSG route. For these purposes, we choose zolmitriptan, a basic drug with pK_a 9.6, as the template. Chiral separation of zolmitriptan has captured great interests [27–32] as only the single (*S*)-enantiomer is effective for acute treatment of severe migraine and related vascular headaches [33–35]. Methods reported for chiral separation of zolmitriptan include either CE with β-CD as chiral additives [27, 28] or HPLC with vancomycin [29, 30] and Chiralpak AD-H [31, 32] as chiral stationary phase. However, no MIPs, to the best of our knowledge, have been reported for the chiral separation of zolmitriptan so far.

To further understand and rationalize the RTIL-mediated NHSG strategy and to realize excellent chiral recognition, two main factors, *i.e.*, the NHSG process and the RTIL (type and amounts) affecting the performance of silica-based hybrid MIP monoliths, are investigated in detail.

2 Materials and methods

2.1 Chemicals and materials

Methacryloxypropyltrimethoxysilane (MPTMS) was from Acros (Geel, Belgium). 1-Butyl-3-methylimidazolium hexafluorophosphate ($BMIM^+PF_6^-$) and 1-butyl-3-methylimidazolium tetrafluoroborate ($BMIM^+BF_4^-$) were synthesized according to the literature [36, 37]. MAA (Beijing Donghuan Chemicals, Beijing, China), trifluoromethyl acrylic acid (TFMAA), and cinnamic acid (Acros) were used as the functional monomers and catalysts of NHSG process. 2,2′-Azobis(2-isobutyronitrile) (AIBN, Fuchen Chemicals, Beijing, China) was used as the radical initiator. (*R*)- and (*S*)-zolmitriptan (Beijing Gao-Bo Pharm-Chemicals, Beijing, China) were recrystallized before use. HPLC-grade ACN (Burdick & Jackson, USA) was used throughout the CEC experiments, and was dried for the preparation of the MIP monoliths. A 50 mM Tris (Beijing Chemicals, Beijing, China)-HCl buffer at pH 5.4 was included in CEC mobile phase. Fused-silica capillaries of 375 μm od × 100 μm id were purchased from Yongnian Optic Fiber Plant (Hebei, China).

2.2 Preparation of MIP monoliths

Before preparation of the monoliths, fused-silica capillaries were pretreated as follows: the capillaries were washed with 1 M NaOH for 2 h, pure water for 30 min, and 0.1 M HCl for 2 h, then washed with pure water again until the outflow reached pH 7.0. The capillaries were dried with nitrogen purging at 150°C in a gas chromatographic oven overnight.

The prepolymerization mixture (see Table 1) was degassed under ultrasonication for 5 min, then the transparent solution was carefully introduced into a pretreated capillary to fill about 28 cm (total length of 40 cm) with a 0.5 mL disposable syringe and both ends were sealed immediately. Subsequently, the 28 cm capillary with prepolymerization mixture was submerged into a 54°C water bath for a period of time (Table 1). Finally, the capillary was moved out of the water bath and immediately flushed with several column volumes of ACN–acetic acid (9:1 v/v) and ACN respectively by a hand-held syringe (the pressures near 200 psi) to remove the unreacted reagents, the RTIL and the imprinting molecule. The nonimprinted polymers were prepared in parallel without addition of zolmitriptan. For FTIR and solid-UV analysis, the imprinted and nonimprinted polymers were also synthesized in sealed bottles (reaction time 72 h) and were dried under vacuum at 80°C for 12 h after Soxhlet extraction by the same extractant as for the monolithic capillaries.

Table 1. Protocol of prepolymerization solutions[a)]

Monolithic column	Acid (mmol)		RTIL[b)] (μL)	Reaction time[c)] (h)
M1	TFMAA	0.11	40	4.5
M2	Cinnamic acid	0.11	40	5
M3	MAA	0.11	40	6
M4	MAA	0.22	40	6
M5	MAA	0.44	40	6
M6	MAA	0.88	40	6
M7	MAA	0.11	0	2.5
M8	MAA	0.11	80	6.3
M9	MAA	0.11	120	6.3
M10	MAA	0.11	40	6

a) ACN was added to ensure a total volume of 1 mL with the same amount of zolmitriptan (0.025 mmol), MPTMS (0.44 mmol), and AIBN (0.027 mmol).
b) RTIL was $BMIM^+PF_6^-$ for M1 to M9 and $BMIM^+BF_4^-$ for M10.
c) Time acquired to obtain permeable column (liquid could be driven through the column at pressures near 200 psi).

2.3 Instrumentation and methods

CEC experiments were performed on a P/ACE MDQ CE system (Beckman-Coulter, Fullerton, CA, USA) equipped with a UV detector. Data acquisition and processing was controlled by Beckman ChemStation software. All the buffers were made using doubly distilled water and filtered before use through a 0.2 μm filter. The monolith was conditioned with the separation mobile phase using a syringe and a hand-held vise. A detection window was created after the monolith section by burning off a 2 mm segment of the polyimide coating. Once fabricated, the capillary was installed in the cartridge without any damage with 20 cm monolith from the inlet to detection window and total length of 31.2 cm (11.2 cm without monolith), and then the monolithic column was further pressure-rinsed (40 psi) and electrokinetically conditioned at 5 kV in the instrument by the separation mobile phase until stable current was obtained. All CEC separation of the ten monoliths was evaluated under the same conditions. Only 5 kV voltage was applied in order to get the chiral separation on all the monoliths as good as possible. The averaged currents of the ten MIP monoliths varied from 6.2 to 11.4 μA during separation (13.5 μA for the raw capillary under the same conditions).

Blank sample (ACN) runs before every sample injection for assurance of no residue interfere. The samples dissolved in ACN and degassed by sonication, were electrokinetically injected, typically at 1 kV for 3 s. UV detection was set at 254 nm.

The values of the separation factor (α) and resolution (R) were calculated according to Eqs. (1) and (2):

$$\alpha = (t_S - t_0)/(t_R - t_0) \quad (1)$$

$$R = (t_S - t_R)/[0.5(w_S + w_R)] \quad (2)$$

where t_R, t_S, and t_0 are the retention times of the (*R*)-, (*S*)-zolmitriptan, and the void marker (thiourea), respectively, w is the width at the baseline between tangents drawn to the inflection points for the peaks. The α and R were used to evaluate the imprinting selectivity of the MIP monolith.

The micrographs of the monoliths were obtained at 15.0 kV on a SS-550 scanning electron microscope (SEM; Shimadzu, Japan). FTIR spectra (4000–400 cm^{-1}) were recorded using a Magna-560 spectrometer (Nicolet, USA). Solid UV spectra (200–800 nm) were obtained using a V-550 spectrometer (JASCO, Japan).

3 Results and discussion

3.1 Fabrication of the RTIL-mediated NHSG hybrid MIP monoliths

The RTIL-mediated NHSG route for the fabrication of molecularly imprinted silica-based hybrid monoliths is based on the reactions of carboxylic acids and siloxanes, both containing a C = C double bond, as illustrated in Scheme 1. Two reactions are involved, one is the free-radical polymerization of the C = C bonds, and the other is the NHSG condensation of the siloxanes catalyzed by the carboxylic acid, the functional monomer for conventional organic-polymer-based MIPs [26].

The protocol of the prepolymerization solutions used to prepare the monoliths is summarized in Table 1. Three kinds of carboxylic acids, namely TFMAA (pK_a 2.1), cinnamic acid (pK_a 4.5) and MAA (pK_a 4.7), were examined as the functional monomer to interact with zolmitriptan noncovalently. These carboxylic acids also acted as the catalysts for the NHSG condensation of MPTMS to form silica-based framework [26, 38–41]. The most commonly used hydrophobic and hydrophilic RTIL, $BMIM^+PF_6^-$, and $BMIM^+BF_4^-$ were incorporated for the purpose to reduce gel shrinkage and also to act as the pore template. Thus, the porous silica-based framework was formed (Fig. 1), and the specific recognition sites for zolmitriptan were left after removing the template (Scheme 1).

The SEM images of the monolith M8 presented in Fig. 1 show a representative morphology of the prepared monoliths. The portrait of the lengthways segment of the monolith shucked off the outer raw capillary displays a continuous porous rod-like materials (Fig. 1a). In addition, the images of the cross-section of the monolith also reveal a continuous porous skeleton morphology (Figs. 1b and c), and as well as the chemical attachment of the monolithic materials to the inner surface of the raw fused-silica capillary (Fig. 1b) owing to the anchors linking of the profuse silanol groups on the inner wall of the capillary after the pretreatment.

FTIR spectra of the $BMIM^+PF_6^-$-mediated zolmitriptan imprinted materials after extraction (Fig. 2A(b)–(d)) display the strong and broad bands around 1164 and 1108 cm^{-1}, which are assigned as the Si–O–Si asymmetric stretching

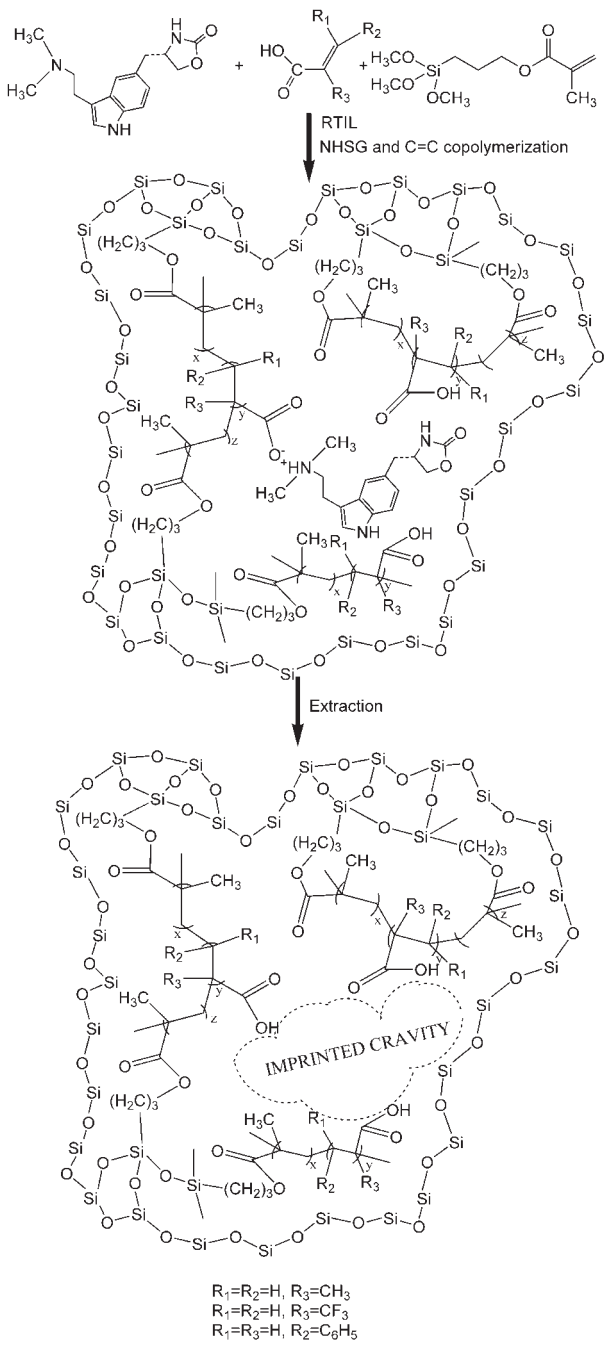

Scheme 1. Scheme and possible mechanism of the RTIL mediated NHSG route to prepare the molecularly imprinted silica-based hybrid monoliths.

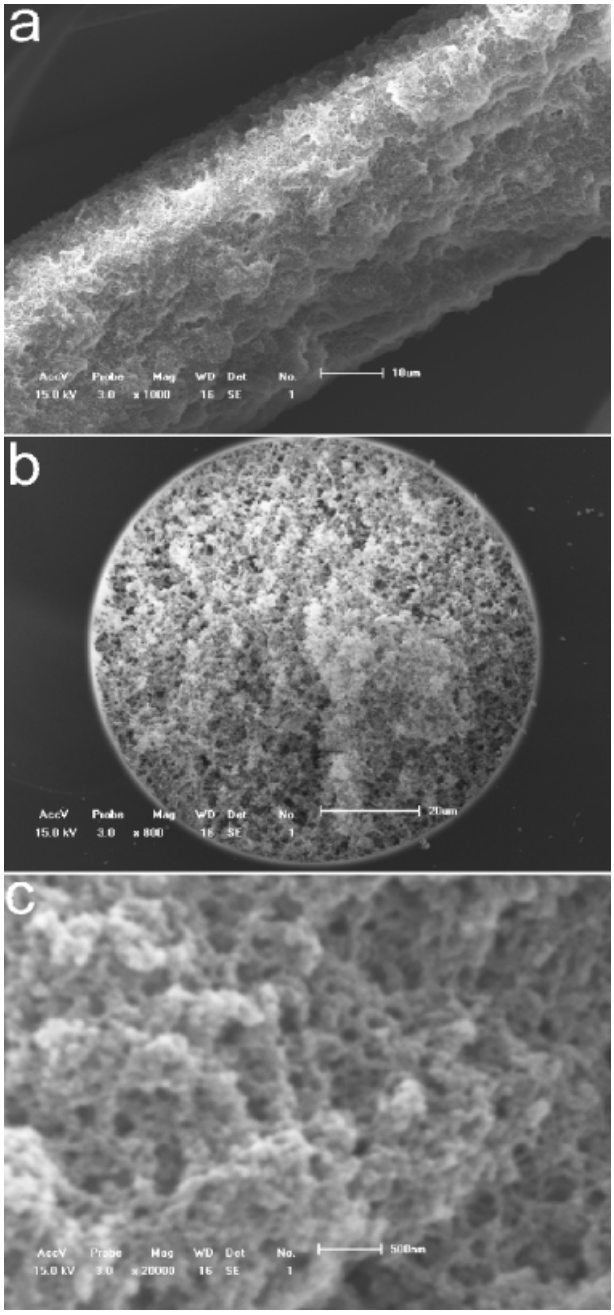

Figure 1. SEM images of the $BMIM^+PF_6^-$-mediated NHSG silica-based hybrid MIP monoliths using MAA as functional monomer (M8): (a) lengthwise segment of the monolith shucked off the outer capillary, (b) cross-section of the monolith magnified 800×, (c) cross-section of the monolith magnified 20 000×.

vibrations. These bands also indicate the formation of the long-chain linear siloxanes [38–39] due to the NHSG condense of MPTMS catalyzed by all the examined carboxylic acids (TFMAA, cinnamic acid, and MAA). The RTIL can be completely removed from the MIPs as the main peaks of Fig. 2A(a) (the FTIR for pure $BMIM^+PF_6^-$) are all absent in Fig. 2A(b)–(d). Removal of the template is an important step in the fabrication of MIPs. In our experiment, the template can also be efficiently removed as the main absorbance of zolmitriptan nearly disappears in the MIPs after extraction (Fig. 2B, the solid-UV spectra of zolmitriptan, the $BMIM^+PF_6^-$-mediated zolmitriptan imprinted polymer M3 before and after extraction).

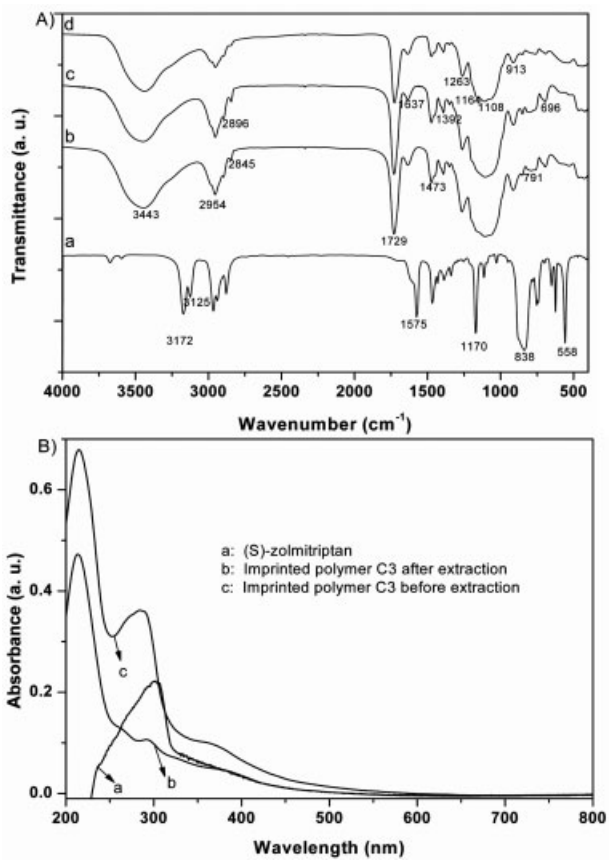

Figure 2. (A) FTIR spectra: (a) $BMIM^+PF_6^-$; (b) $BMIM^+PF_6^-$-mediated zolmitriptan imprinted hybrid polymers using TFMAA as functional monomers after extraction (M1); (c) $BMIM^+PF_6^-$-mediated zolmitriptan imprinted hybrid polymers using cinnamic acid as functional monomers after extraction (M2); (d) $BMIM^+PF_6^-$-mediated zolmitriptan imprinted hybrid polymers using MAA as functional monomers after extraction (M3). (B) Solid-state UV spectra of zolmitriptan, and $BMIM^+PF_6^-$-mediated zolmitriptan imprinted polymer using MAA as functional monomer (M3) after and before extraction.

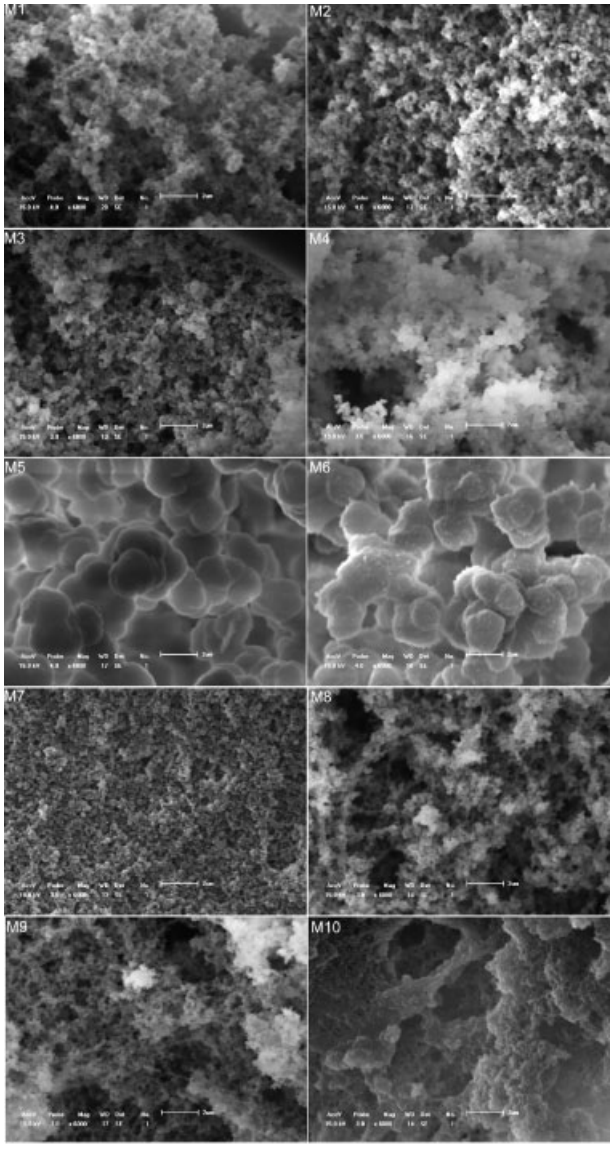

Figure 3. SEM images of the cross-sections of the prepared MIP monoliths M1 to M10 after extraction magnified 6000 ×. M1, M2, and M3 were prepared using TFMAA, cinnamic acid, and MAA, respectively. Monoliths M3 to M6 were compared to display the effect of the amount of MAA. M3 and M10 were synthesized in the presence of $BMIM^+PF_6^-$ and $BMIM^+BF_4^-$, respectively. M7, M3, M8, and M9 were compared to show the effect of the content of $BMIM^+PF_6^-$ (0, 40, 80, and 120 μL). Detail conditions for the preparation of monoliths M1 to M10 are summarized in Table 1.

3.2 Effect of carboxylic acids

It follows from the previous section that two reactions were involved in the RTIL-mediated NHSG methodology, *i.e.*, the free-radical copolymerization of the C = C bond and the NHSG condense of the siloxane catalyzed by the carboxylic acids [26]. The free-radical copolymerization is a faster reaction, while the so-called NHSG process is slower (approximately half of the tetramethyl orthosilicate converted to various silicate species catalyzed by MAA over about 190 h at 55°C) [41]. Despite the copolymerization of different carboxylic acids and the siloxane had different reaction rate, the overall reaction time lied on the NHSG process.

As Table 1 shows, stronger carboxylic acid resulted in shorter reaction time for the NHSG process (M1–M3, 4.5 h for TFMAA, 5 h for cinnamic acid and 6 h for MAA) since stronger carboxylic acid could cause the siloxane to lost alcohols more easily [41]. As large surface of the 28 cm capillary (375 μm od × 100 μm id) used in the present work with prepolymerization mixture in a 54°C water bath benefited the homogeneous reaction, and the synergism of the free-radical copolymerization existed, the reaction time in the present NHSG process was much shorter than that reported [41]. The synergism of the free-radical copolymerization was

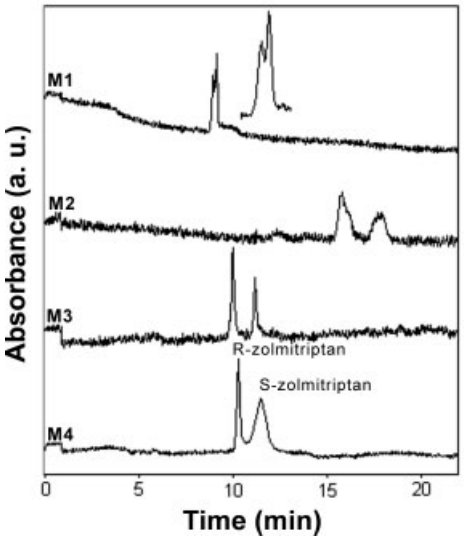

Figure 4. Electrochromatograms of the (*R*)/(*S*)-zolmitriptan mixture on the $BMIM^+PF_6^-$-mediated zolmitriptan-imprinted monoliths M1 to M4, showing the effect of carboxylic acids. The CEC separations were performed at an applied voltage 5 kV with an overpressure of 30 psi at 25°C using a mixture of ACN and Tris-HCl (50 mM, pH 5.4) as the mobile phase (70:30 v/v). The analyte solution was electrokinetically injected at 1 kV for 3 s and detected at 254 nm with a UV detector. The separation factor (α) and resolution (*R*) of M1 to M4 was: M1 $\alpha = 1.03$, $R = 0.68$; M2 $\alpha = 1.49$, $R = 1.83$; M3 $\alpha = 1.34$, $R = 4.26$; M4 $\alpha = 1.29$, $R = 1.83$. For other conditions see Table 1.

ascertained by the fact that the reaction time was almost the same in the preparation of the monoliths M3 to M6 as the concentration of MAA increased (Table 1). If the free-radical copolymerization did not exist, the NHSG reaction should be faster as the concentration of the catalyst increased. However, in the present NHSG process the free-radical copolymerization of MAA and MPTMS would lead to the rearrangement of the trimethoxysilylpropyloxy group of MPTMS. If the amount of MAA increased, the density of the trimethoxysilylpropyloxy group would be reduced or the distance of that group increased, thus the NHSG condense would be slowed. Consequently, the reaction time for the present NHSG process was almost independent of MAA concentration.

The synergism of the free-radical copolymerization was further supported by the morphology revealed by the SEM images (M3–M6, Fig. 3). Smaller amount of MAA was favorable for the formation of monoliths with smaller particle size (<200 nm for M3 and <400 nm for M4), whereas larger amount of MAA resulted in larger particles (~2 μm for M5 and M6). Larger amount of MAA would result in the farther distance of the trimethoxysilylpropyloxy group of MPTMS (Scheme 1, $y \geq 2$), and thus larger particle sizes of M5 and M6. Moreover, the large particles of M6 were less homogenous compared to M5 due to stochastic copolymerization of MAA and MPTMS, and small protuberance might result from the puckered polymerized MAA.

Although the nature of the carboxylic acid insignificantly affected the morphology of the prepared monoliths M1 to M3 (Fig. 3), the chiral recognition abilities of the three monoliths prepared with various carboxylic acids were notably different (M1–M3, Fig. 4). The (*R*)/(*S*)-zolmitriptan was baseline-separated when MAA and cinnamic acid were used, whereas two enantiomers were partly resolved in the case of TFMAA. The propulsion of the mobile phase, EOF of the monoliths from M1 to M3 were 4.9, 1.8, and $3.1 \times 10^{-8}\ m^2 \times v^{-1} \times s^{-1}$, respectively (all conditions as in Fig. 4), which is in good agreement with the fastest elution of the analytes on monolith M1 and the lowest elution on monolith M2 (Fig. 4). The denser morphology of the monolith M2 (M2, Fig. 3) and the stronger hydrophobic interactions of the phenyl group of polymerized cinnamic acid and the analytes were also the reasons for the longest retention time of (*R*)/(*S*)-zolmitiptan on the monolith M2.

The monoliths M3 to M6 were compared to elucidate the marked effect of the amount of MAA. Except for the above-mentioned notable difference in topography of the monoliths M3 to M6, great difference in CEC performance was also observed for these monoliths. The current, as well as the EOF in CEC experiments were not stable for M5 and M6, so no electrochromatograms were given for these two monolithic columns. However, the monolithic columns M3 and M4 offered excellent CEC performance, and baseline separation of the (*R*)/(*S*)-zolmitriptan mixture (M3–M4, Fig. 4). These phenomena can be ascribed to the copolymerization of the excess MAA and MPTMS, which leads to the heterogeneous hybrids of organic and inorganic segments with the reduced silica matrix.

3.3 Role of RTIL

RTIL has been used in recent studies in the area of structural materials science as the pore templates and cosolvents in the synthesis of mesoporous and microporous materials, areogels, and functionalized sol–gels [25, 42–47]. RTIL has also been found to accelerate synthesis and improve selectivity of the *trans*-aconitic imprinted polymers (organic-polymer-based) [48]. In our latest communication, we have incorporated RTIL in the preparation of (*S*)-naproxen imprinted silica-based monoliths by the RTIL-mediated NHSG methodology [26]. However, the exact role of the RTIL is indistinct. In the present work the effect of RTIL (type and volume) was investigated in details for deeper understanding of the role of RTIL.

The monoliths M7 (without RTIL), M3 (with 40 μL $BMIM^+PF_6^-$) and M10 (with 40 μL $BMIM^+BF_4^-$) are compared to elucidate the great differences in morphology and CEC performance between the monoliths prepared with and without RTIL. The (*R*)/(*S*)-zolmitriptan was only partly

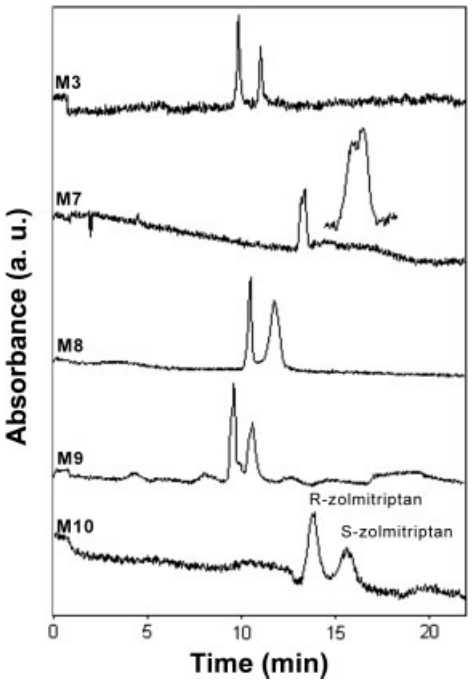

Figure 5. Electrochromatograms of the (*R*)/(*S*)-zolmitriptan mixture on the zolmitriptan-imprinted monoliths M3 and M7 to M10, showing the effect of RTIL. The CEC separations were performed at an applied voltage 5 kV with an overpressure of 30 psi at 25°C using a mixture of ACN and Tris-HCl (50 mM, pH 5.4) as the mobile phase (70:30 v/v). The analyte solution was electrokinetically injected at 1 kV for 3 s and detected at 254 nm with a UV detector. The separation factor (α) and resolution (R) of M3 and M7 to M10 was: M3 $\alpha = 1.34$, $R = 4.26$; M7 $\alpha = 1.03$, $R = 0.53$; M8 $\alpha = 1.25$, $R = 2.11$; M9 $\alpha = 1.24$, $R = 1.71$; M10 $\alpha = 1.32$, $R = 1.62$. For other conditions see Table 1.

resolved on the monolithic column without RTIL incorporated, whereas baseline separation of (*R*)/(*S*)-zolmitriptan was achieved on the column in the presence of 40 μL of $BMIM^+PF_6^-$ or $BMIM^+BF_4^-$ (M7 *vs.* M3, M7 *vs.* M10, Fig. 5). The effective column porosity ε calculated according to the reported method [49] and SEM images might reveal the reason for the great discriminations of the recognition selectivity between these columns. When no RTIL was involved, the monolithic rod was less porous (M7 ($\varepsilon = 0.48$), Fig. 3), which was responsible for the poor recognition ability, since less porosity led to less chances for the analytes to access the recognition site. When small amounts of RTIL were incorporated, a higher porous network was formed (M3 ($\varepsilon = 0.61$) and M10 ($\varepsilon = 0.70$), Fig. 3), thus the recognition selectivity was enhanced. Although the recognition selectivity was significantly improved as the RTIL was involved, the reaction time was prolonged. When no RTIL was incorporated (M7), the reaction time was shorter, whereas when 40 μL of $BMIM^+PF_6^-$ (M3) or 40 μL of $BMIM^+BF_4^-$ (M10) was added, the reaction time was much longer (Table 1). The difference in reaction time can also be attributed to the increased distance of the trimethoxysilylpropyloxy group of MPTMS as the RTIL was incorporated owing to the interactions of the RTIL and the siloxane [25, 39, 45]. Although the high ionic strength of the RTIL could result in faster aggregation [42–43], the farther distance of the trimethoxysilylpropyloxy group of MPTMS would prolong the reaction time. However, the particles were not enlarged owing to the pore forming by the RTIL.

Although the baseline separation was achieved on the monoliths prepared in the presence of different kinds of RTIL (M3 *vs.* M10, Fig. 5), the retention times of the analytes were prolonged as $BMIM^+BF_4^-$ was used (M10), which is in good agreement with the slower EOF of M10 ($2.5 \times 10^{-8}\ m^2 \times v^{-1} \times s^{-1}$). The use of identical volume of $BMIM^+PF_6^-$ and $BMIM^+BF_4^-$ did not significantly influence the reaction time needed to obtain permeable monolithic column (M3 *vs.* M10, Table 1), but resulted in remarkable different morphology of these two monoliths (M3 *vs.* M10, Fig. 3). Incorporation of $BMIM^+BF_4^-$ gave the monolith with porous blocks (M10, Fig. 3), whereas $BMIM^+PF_6^-$ resulted in the monolith with particles network (M3, Fig. 3), which might be owing to the stronger hydrogen bonding of BF_4^- and silanol groups compared to PF_6^- and silanol groups [39, 45].

The monoliths M3 (40 μL), M8 (80 μL), and M9 (120 μL) were prepared with the increased volume of $BMIM^+PF_6^-$ to investigate the effect of the volume of RTIL. Increase of the volume of $BMIM^+PF_6^-$ slightly prolonged the reaction time (M3 *vs.* M8 and M9, Table 1) and led to a little decrease of selectivity (M3 *vs.* M8 *vs.* M9, Fig. 5). However, baseline separation of (*R*)/(*S*)-zolmitriptan was still observed on these columns (M8 and M9, Fig. 5). SEM images reveal different morphology of these monoliths. When small amount of $BMIM^+PF_6^-$ was incorporated, a porous network with larger pores was formed (M3 *vs.* M8 *vs.* M9, Fig. 3). As the amounts of $BMIM^+PF_6^-$ were further increased, the formation of smaller pores became more dominant and a more uniform topography with much smaller pores and a smaller pore size distribution was observed, but ultimately the porosity was increased (M8 ($\varepsilon = 0.75$) and M9 ($\varepsilon = 0.85$), Fig. 3), which is in accordance with the observations in the literature [25] and was consistent with the faster elution of the analytes on this monolith. As expected, the selectivity was decreased due to less interaction of the analytes and the recognition sites.

4 Concluding remarks

We have demonstrated successful fabrication of new molecularly imprinted silica-based hybrid monoliths for chiral recognition of a basic drug, zolmitriptan, by the RTIL-mediated NHSG methodology, and provided new insights into the mechanism of the RTIL-mediated NHSG route. The synergism of free-radical copolymerization of carbon–carbon double bond of the carboxylic acids and siloxanes with NHSG

condense of the siloxanes catalyzed by the same carboxylic acid was proposed since the free-radical copolymerization was usually faster, leading to the rearrangement of the $-Si(OR)_3$ group and affecting the NHSG condensation. Other evidences, such as the real time FT-IR of C=C bond and MAS ^{29}Si NMR study [50], would benefit further understanding of the mechanism of the RTIL-mediated NHSG route. Incorporation of RTIL increased the porosity, and hence improved the selectivity of the prepared hybrid monoliths. We expect that the RTIL-mediated NHSG protocol is promising as a general strategy for the fabrication of high selective imprinted hybrid materials for molecular recognition.

This work was supported by the 863 Program (no. 2007AA10Z432), the National Basic Research Program of China (no. 2006CB705703), and the National Natural Science Foundation of China (no. 20705013).

The authors have declared no conflict of interest.

5 References

[1] Berthod, A., *Anal. Chem.* 2006, *78*, 2093–2099.

[2] Ward, T. J., *Anal. Chem.* 2006, *78*, 3947–3956.

[3] Sellergren, B., *Molecularly Imprinted Polymers: Man-Made Mimics of Antibodies and Their Applications in Analytical Chemistry*, Elsevier, New York 2001.

[4] Wulff, G., *Angew. Chem. Int. Ed.* 1995, *34*, 1812–1832.

[5] Mosbach, K., Ramström, O., *Biotechnology* 1996, *14*, 163–170.

[6] Wistuba, D., Schurig, V., *J. Chromatogr. B* 2000, *875*, 255–276.

[7] Kempe, M., Mosbach, K., *J. Chromatogr. A* 1995, *694*, 3–13.

[8] Schweitz, L., Spegel, P., Nilsson, S., *Electrophoresis* 2001, *22*, 4053–4063.

[9] Turiel, E., Martin-Esteban, A., *J. Sep. Sci.* 2005, *28*, 719–728.

[10] Nilsson, J., Spegel, P., Nilsson, S., *J. Chromatogr. B* 2004, *804*, 3–12.

[11] Liu, Z.-S., Zheng, C., Yan, C., Gao, R.-Y., *Electrophoresis* 2007, *28*, 127–136.

[12] Qin, F., Xie, C., Yu, Z., Kong, L. *et al.*, *J. Sep. Sci.* 2006, *29*, 1332–1343.

[13] Yu, C., Mosbach, K., *J. Chromatogr. A* 2000, *888*, 63–72.

[14] Burleigh, M. C., Dai, S., Hagaman, E. W., Lin, J. S., *Chem. Mater.* 2001, *13*, 2537–2546.

[15] Dai, S., Burleigh, M. C., Ju, Y. H., Gao, H. J. *et al.*, *J. Am. Chem. Soc.* 2000, *122*, 992–993.

[16] Makote, R. D., Dai, S., *Anal. Chim. Acta* 2001, *435*, 169–175.

[17] Graham, A. L., Carlson, C. A., Edmiston, P. L., *Anal. Chem.* 2002, *74*, 458–467.

[18] Makote, R., Collinson, M. M., *Chem. Mater.* 1998, *10*, 2440–2445.

[19] Dai, S., Burleigh, M. C., Shin, Y., Morrow, C. C. *et al.*, *Angew. Chem. Int. Ed.* 1999, *38*, 1235–1239.

[20] Hunnius, M., Rufińska, A., Maier, W. F., *Microporous Mesoporous Mater.* 1999, *29*, 389–403.

[21] Lu, Y.-K., Yan, X.-P., *Anal. Chem.* 2004, *76*, 453–457.

[22] Fang, G.-Z., Tan, J., Yan, X.-P., *Anal. Chem.* 2005, *77*, 1734–1739.

[23] Siouffi, A.-M., *J. Chromatogr. A* 2003, *1000*, 801–818.

[24] Ou, J., Li, X., Feng, S., Dong, J. *et al.*, *Anal. Chem.* 2007, *79*, 639–646.

[25] Klingshirn, M. A., Spear, S. K., Holbrey, J. D., Rogers, R. D., *J. Mater. Chem.* 2005, *15*, 5174–5180.

[26] Wang, H.-F., Zhu, Y.-Z., Yan, X.-P., Gao, R.-Y., Zheng, J.-Y., *Adv. Mater.* 2006, *18*, 3266–3270.

[27] Yang, G. L., Liu, Y., Song, X. R., Chen, Y., *Chin. J. Anal. Chem.* 2003, *31*, 1149.

[28] He, M., Xia, Z.-N., Liu, Y., Xiang, S.-F., Li, G. R., *Chin. J. Pharm. Anal.* 2002, *22*, 438–440.

[29] Zhang, D., Xu, X., Ma, S., *J. Sep. Sci.* 2005, *28*, 2501–2504.

[30] Ding, G., Liu, Y., Cong, R., Wang, J., *Chin. J. Chromatogr.* 2004, *22*, 386–389.

[31] Yu, L., Yao, T., Ni, S., Zeng, S., *Biomed. Chromatogr.* 2005, *19*, 191–195.

[32] Srinivasu, M. K., Mallikarjuna Rao, B., Sridhar, G., Rajender Kumar, P. *et al.*, *J. Pharm. Biomed. Anal.* 2005, *37*, 453–460.

[33] Yates, R., Niam, K., Dixon, R., Kemp, J. V., Dane, A. L., *J. Clin. Pharmacol.* 2002, *42*, 1244–1250.

[34] Cittadini, E., May, A., Straube, A., Evers, S. *et al.*, *Arch. Neurol.* 2006, *63*, 1537–1542.

[35] Syrett, N., Abu-Shakra, S., Yates, R., *Neurology* 2003, *61*, S27–S30.

[36] Huddleston, J. G., Willauer, H. D., Swatloski, R. P., Visser, A. E., Rogers, R. D., *Chem. Commun.* 1998, 1765–1766.

[37] Xu, D.-Q., Liu, B.-Y., Luo, S.-P., Xu, Z.-Y., Shen, Y.-C., *Synthesis* 2003, *17*, 2626–2628.

[38] Green, W. H., Le, K. P., Grey, J., Au, T. T., Sailor, M. J., *Science* 1997, *276*, 1826–1828.

[39] Liu, Y., Wang, M., Li, Z., Liu, H. *et al.*, *Langmuir* 2005, *21*, 1618–1622.

[40] Sharp, K. G., *J. Sol-Gel Sci. Technol.* 1994, *2*, 35–41.

[41] Skrdla, P. J., Shnayderman, M., Wright, L., O'Brien, T. P., *J. Non-Cryst. Solids* 2006, *352*, 3302–3309.

[42] Yoo, K., Choi, H., Dionysiou, D. D., *Chem. Commun.* 2004, 2000–2001.

[43] Dai, S., Ju, Y. H., Gao, H. J., Lin, J. S. *et al.*, *Chem. Commun.* 2000, 243–244.

[44] Lee, B., Luo, H., Yuan, C. Y., Lin, J. S., Dai, S., *Chem. Commun.* 2004, 240–241.

[45] Zhou, Y., Schattka, J. H., Antonietti, M., *Nano. Lett.* 2004, *4*, 477–481.

[46] Zhou, Y., Antonietti, M., *Chem. Mater.* 2004, *16*, 544–550.

[47] Néouze, M.-A., Le Bideau, J., Leroux, F., Vioux, A., *Chem. Commun.* 2005, 1082–1084.

[48] Booker, K., Bowyer, M. C., Holdsworth, C. I., McCluskey, A., *Chem. Commun.* 2006, 1730–1732.

[49] Chen, L., Chen, L., Yan, X., Wan, Q.-H., *Anal. Chem.* 2002, *74*, 5157–5159.

[50] Soppera, O., Croutxé-Barghorn, C., Lougnot, D. J., *New J. Chem.* 2001, *25*, 1006–1014.

